Structure of solvated mercury(II) halides in liquid ammonia, triethyl phosphite and tri-*n*-butylphosphine solution

Kersti B. Nilsson,[a] Mikhail Maliarik,[b] Ingmar Persson[a*] and Magnus Sandström[c]

[a] Department of Chemistry, Swedish University of Agricultural Sciences, P.O.Box 7015, SE-750 07 Uppsala, Sweden.

[b] IFM - Department of Chemistry, Linköping University, SE-581 83 Linköping, Sweden

[c] Department of Physical, Inorganic and Structural Chemistry, Stockholm University, SE-106 91 Stockholm, Sweden.

Supporting Material

Table S1. Raman frequencies with assignments of mercury(II) halides in liquid ammonia solutions and solid ammonia solvated mercury(II) halide compounds.[a]

Solvate complex / Solute in liquid ammonia	ν_s(Hg-X)	ν_s(Hg-N)	$\rho_r(NH_3)$	$\delta_s(NH_3)$	$\delta_d(NH_3)$	$2\delta_d(NH_3)$	$\nu_s(NH_3)$	$\nu_a(NH_3)$
$[Hg(NH_3)_4]^{2+}$ / $HgCl_2$ (light phase)				1060 w,br	1634 w	3215 vs	3295 vs	3370 m
$[Hg(NH_3)_4]^{2+}$ / $HgCl_2$ (dense phase)		405 vs		1101 w,br 1225 w,br	1634 m	3213 vs	3292 s,sh	3354 m
$[Hg(NH_3)_2]Cl_2$ (*s*)		378 vs 415 m,sh 450 m,sh	685 m,br	1260 s	1598 m,br	3211 s 3143 m,sh		
$[Hg(NH_3)_4]^{2+}$ / $HgBr_2$				1100 m,br		3213 vs	3295 s	
$[Hg(NH_3)_2]Br_2$ (*s*)		378 vs 415 m,sh	691 m,br	1261 s	1591 m,br	3211 s 3140 m,sh		
$[HgI_2(NH_3)_2]$ / HgI_2	132 vs	356 m,br		1060 w,br 1205 w,br	1636 w	3213 vs	3298 vs	3375 m
$HgI_2(NH_3)_2$(*s*)[b]	116 vs 130 vs	378 vs 415 m,sh 450 w,sh		1260 w,br	1588 m	3211 s 3138 m,sh		3375
$[HgI_4]^{2+}$ / $Hg(ClO_4)_2$, NH_4I	121 vs			1105 m	1620 m	3212 s	3286 s	3360 m
NH_3 (l)				1055 w,br	1642 m	3215 vs	3295 vs	3385 m

[a] Abbreviations: vs very strong, s strong, m medium, w weak, br broad, sh shoulder

[b] Decomposes rapidly in air giving red mercury(II) iodide after a few minutes.

Legends to Figures

Figure S1. Normalised XANES spectra of the analysed mercury(II) halides: (a) $[Hg(NH_3)_4]^+$ (from $HgBr_2$ in NH_3(l); no offset), (b) $[Hg(NH_3)_4]^+$ (from $HgCl_2$ in $NH_3(l)$, light phase; offset 0.25), (c) $[Hg(NH_3)_4]^+$ (from $Hg(ClO_4)_2$ in $NH_3(l)$, offset 0.7) and (d) $[HgI_4]^{2-}$ in $NH_3(l)$; offset 1.0).

Figure S2. Fourier Transforms of the experimental (thin solid line) and theoretical model (thick solid line) data of the analysed mercury(II) complexes : $[Hg(NH_3)_4]^{2+}$ (from $HgBr_2$ in $NH_3(l)$; no offset), $[Hg(NH_3)_4]^{2+}$ (from $HgCl_2$ in $NH_3(l)$, light phase; offset +0.2) and $[HgI_4]^{2-}$ in $NH_3(l)$; offset +0.6).

Figure S3. Curve fitting of the high frequency part of the Raman spectrum of the dense phase of the three-phase $HgCl_2$-$NH_3(l)$ system. Experimental spectrum (black), individual bands (green), fitted spectrum (red).

Figure S4. Raman spectrum of the light phase of the three-phase $HgCl_2$-$NH_3(l)$ system (red) and the liquid ammonia solution of $HgBr_2$ (black).

Figure S5. Raman spectrum of the solution of the tetraiodomercurate(II) complex in liquid ammonia.

Figure S1.

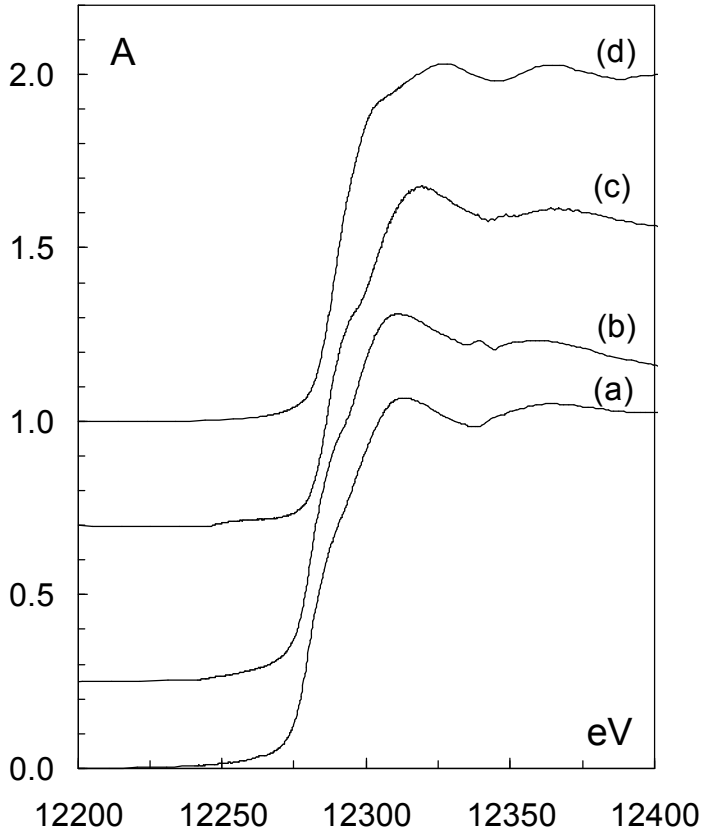

Figure S2.

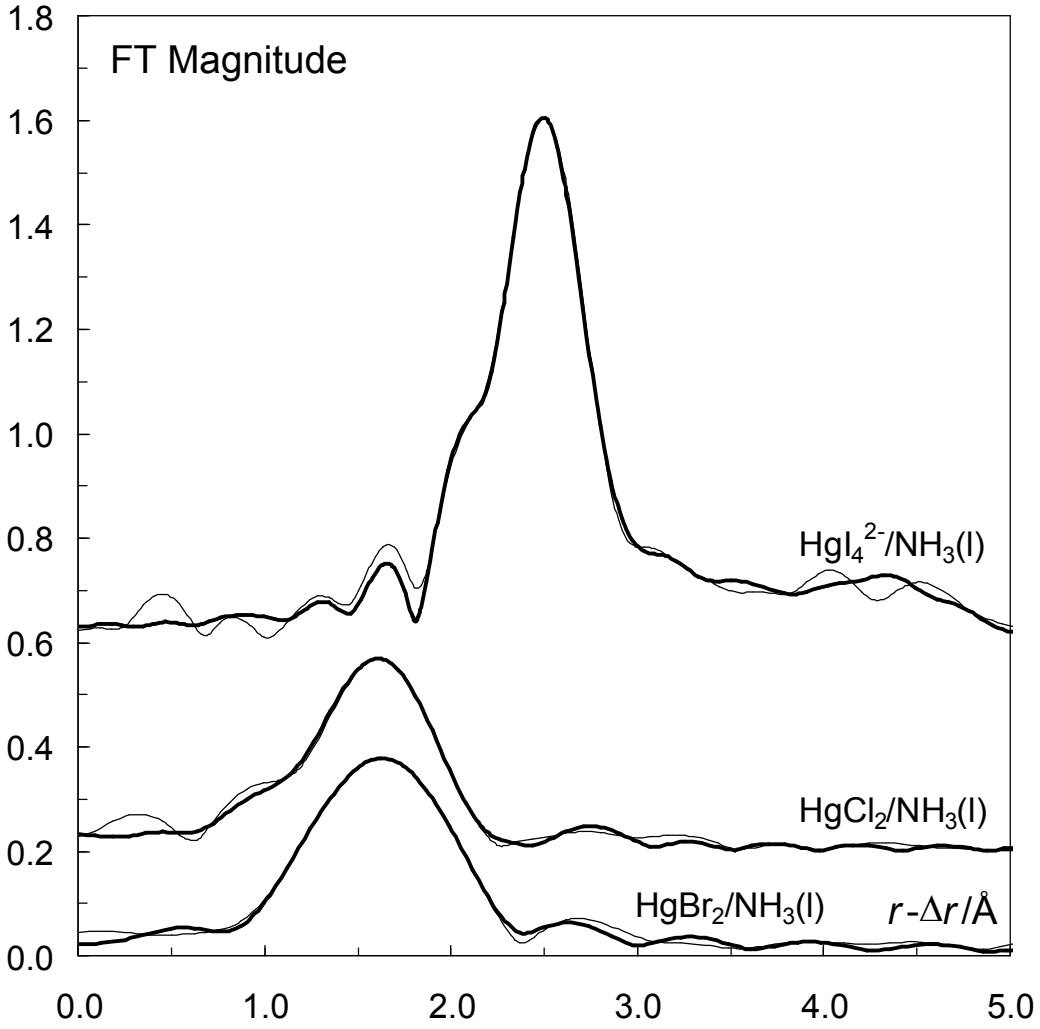

Figure S3.

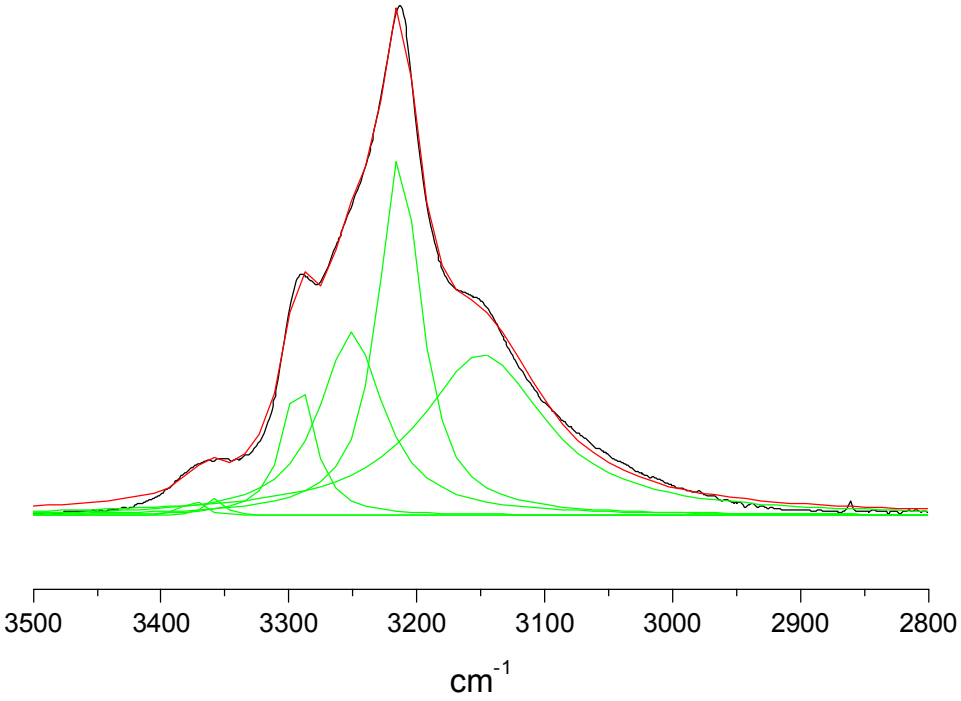

Figure S4.

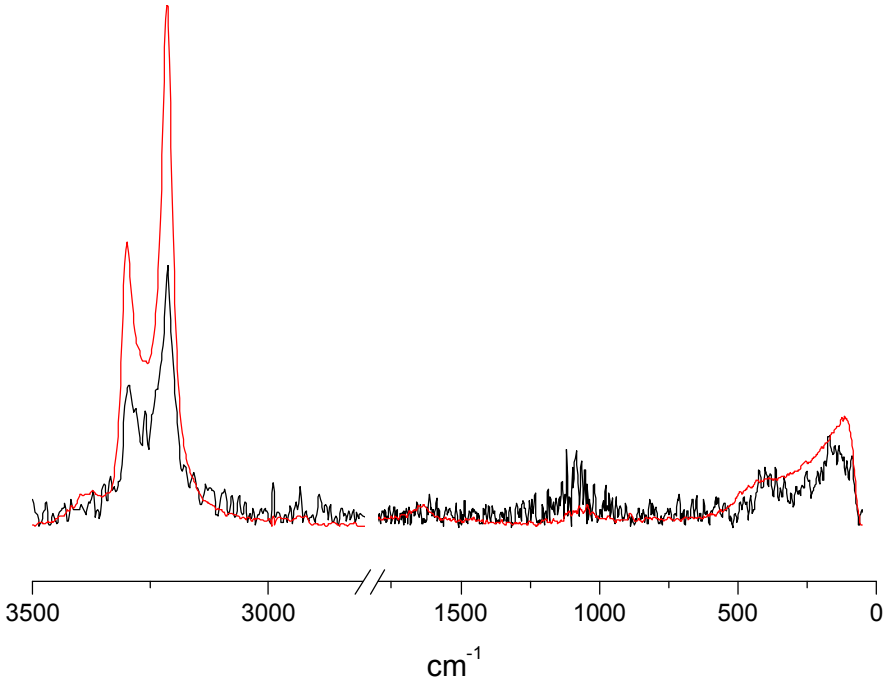

Figure S5.